American Journal of Signal Processing 2025, 13(1): 1-16
DOI: 10.5923/j.ajsp.20251301.01

Machine Learning-Based Fault Diagnosis and Characterization System for Power-Generating Sets Using Customized Fault Audio Dataset

Ekerette Ibanga*, Kingsley Udofia, Kufre Udofia, Unwana Iwok, Emmanuel Ogungbemi

Department of Electrical and Electronics Engineering, Faculty of Engineering, University of Uyo, Uyo, Nigeria

Abstract The growing dependency on stable power supply has made unexpected downtime a dreaded event. Research in Signal processing and machine learning techniques have become hot areas for the diagnosis of faults in power-generating systems due to their advantages, which include fast diagnosis, high detection accuracy, good generalization, and low cost. The focus of this work is to use a customized dataset to develop a machine learning-based system for fault diagnosis in selected domestic power-generating sets. The approach analyses the unique sound patterns associated with each fault type for twenty-five 5kVA generators under five distinct operational conditions: carburetor fault, exhaust blockage, loose valve, weak Plug, and normal. Signals were pre-processed, normalized and discriminative features extracted and converted to numerical representations of the fault audio patterns. The Support Vector Machines (SVC), random forest, and K-Nearest Neighbours (KNN) supervised machine learning algorithms were trained on the annotated feature datasets and classified for the type of fault. The performance of each model was evaluated using key performance metrics, including accuracy, precision, recall, and F1-score, with k-fold cross-validation (k=10) to ensure generalizability, as well as a confusion matrix to derive performance measures for each condition. Before hyper-parameter tuning, these models achieved accuracies of 85%, 82%, and 83%, respectively. Notably, SVC demonstrated a significant improvement post-tuning, with accuracy increasing by 4.8% to 87%. In contrast, Random Forest showed a slight increase of 0.47%, while KNN showed no improvement. The results from the confusion matrices showed better classification performance for SVC compared to KNN and Random Forest. This indicates that SVC is most suitable for real-time deployment in fault diagnosis of generator systems based on audio signals.

Keywords Machine learning, Fault diagnosis, Signal processing, Feature extraction, Power generator faults

1. Introduction

Power-generating systems, which include equipment such as diesel or petrol generators, wind turbines, hydroelectric generators, and solar power inverters, are essential for the continuous supply of electricity, supporting a wide range of applications from large-scale industrial operations to individual households. With the demand for stable electricity, it becomes necessary to operate these systems online. Early and effective fault diagnoses can mitigate the risks associated with power system failures [1] [2] and ensure optimal performance. A system that automatically collects signal data processes it, classifies the data, and diagnoses the fault can provide security in the surveillance of critical assets, such as electrical substations and industrial scenarios, reduce downtime of machines, decrease maintenance costs, and avoid devastating accidents [3].

* Corresponding author:
ebibanga@gmail.com (Ekerette Ibanga)
Received: Jul. 10, 2025; Accepted: Aug. 3, 2025; Published: Aug. 8, 2025
Published online at http://journal.sapub.org/ajsp

The power generator comprises six subsystems: the stator winding, rotor winding, stator core, mechanical components, cooling system, and excitation system. Faults can be mechanical wear and component degradation arising from worn-out bearings, misaligned shafts, or lubrication failure, electrical imbalances such as voltage imbalances, short-circuit faults, or faults in the alternator, thermal stresses, which typically manifest as overheating affecting critical components such as turbines, engines, or cooling systems. To avoid costly downtime, extensive repairs, and, in extreme cases, system failure, fault diagnosis systems should be implemented promptly [4] [5] to determine which subsystem is affected and which type of failure is present. Fault diagnosis in power-generating systems has historically progressed from manual inspections and simple monitoring techniques to traditional methods, including vibration analysis and thermal imaging, which have high installation costs and are affected by surrounding equipment, leading to poor diagnostic accuracy and reliability [6]. These traditional methods were the primary source of signal capture for data-driven methodologies, which were prone to human error and inefficiency, particularly in complex systems operating under dynamic conditions, resulting in delayed fault detection and reactive maintenance. This led to an increased risk of catastrophic failures and extended downtime of critical equipment [7] [8]. However, sound sensors that capture acoustic sound signals are becoming increasingly popular for fault diagnosis over conventional vibration sensors [9].

Current mechanical fault diagnosis technology is based on the analysis of signals, such as vibration signals [10], force signals, and audio signals. This is because acoustic sensor-based monitoring is an emerging area of interest due to its ability to accurately capture fault signatures and improve the detection accuracy of system anomalies [9]. This fault diagnosis approach utilizes audio-digital processing and transformation techniques to extract valuable information about the system's internal state from the unique acoustic signatures generated by distinct faults. These signals, generated by machinery during both normal and faulty operations, are captured and analyzed to identify specific issues within the system. This signal-based fault diagnosis method offers benefits such as high precision, low cost, great generalizability, and non-contact measurement. Examples of audio signal analysis methods include Fourier Transform, wavelet analysis [11], and Short-Time Fourier Transform (STFT) [12] [2].

In addition to signal processing techniques, the application of machine learning algorithms, including Support Vector Machines (SVMs) and Artificial Neural Networks (ANNs) [13], as well as tree-based classifiers, has revolutionized the diagnosis of faults in machinery.

The use of audio signal processing combined with machine learning for fault diagnosis introduces several novel aspects compared to traditional methods (e.g., vibration analysis, thermal imaging, or manual inspection). It provides non-contact, non-intrusive monitoring with less expensive and minimal hardware. Fault patterns are detected early and in real-time by the models, thus improving preventive maintenance. It is computationally inexpensive and is suitable for remote, rural, or developing regions. The customized audio dataset, tailored to specific power-generating systems, introduces domain-specific intelligence and enables more accurate and context-aware models, rather than generalized diagnostic systems. The introduction of additional sensor capabilities enables a hybrid system for enhanced fault diagnosis.

Collecting data is necessary to integrate machine learning algorithms into fault diagnosis, enabling fast and accurate real-time fault detection, which translates to reduced downtime. [14] However, it can be challenging to distinguish between primary data and noise, as the acquired data often contains noise from the surrounding environment that is processed in subsequent stages. Identifying fault issues in power-generating sets is a challenge in modelling where no prior knowledge of the unique characteristics of failure conditions exists for the machine case study. This can ultimately degrade the model's performance by yielding inaccurate fault diagnosis. [9]. Traditional fault diagnosis methods are plagued by problems, including time-consuming practices, labor-intensive processes, and susceptibility to errors, leading to prolonged downtime and increased operational costs.

This research aims to address these challenges by developing a robust fault diagnosis system that integrates audio processing with machine learning techniques to enable the real-time identification and categorization of faults in power-generating systems.

The contributions of this work are as follows:-

i. Provides statistical data associated with each type of fault for the selected power-generating sets.
ii. Pre-process and annotate recorded audio data from the selected power-generating systems under diverse fault conditions.
iii. Leveraging audio signal processing tools such as mel-frequency cepstral coefficients (MFCC), continuous wavelet transform (CWT), and short-time Fourier transform (STFT) for the extraction of features that capture the unique acoustic signatures associated with selected fault conditions.
iv. To utilize data-driven machine learning methods, such as KNN, SVC, and Random Forest, in fault classification and diagnosis for select power-generating systems.
v. To evaluate the performance of the machine learning models in fault diagnosis of the selected power-generating sets.
vi. To conduct real-time testing of the developed fault detection and characterization system under real-world operating conditions.

This study focuses on audio samples recorded from 25 5kVA petrol-power generating systems under controlled settings and with respect to four fault conditions compared to normal conditions. The fault conditions considered include carburetor issues, exhaust problems, valve malfunctions, spark plug faults, and normal operational states. This scope reduces the system's applicability to a broader spectrum of potential faults commonly found in power-generating sets. The system relies solely on audio signals for fault detection. Hence, faults that do not produce distinctive acoustic signatures or are masked by ambient noise may go undetected. The system is designed for closed-set fault classification, where all possible fault conditions are pre-defined and may struggle with open-set fault diagnosis.

2. Literature Review

Fault diagnosis in power-generating systems involves identifying and characterizing fault issues and is critical to ensuring the reliable operation of power-generating sets. A stable power supply is essential in various sectors because faults degrade efficiency, causing increased fuel consumption, reduced output, and higher operational costs [15] [16].

Predictive maintenance (PdM) techniques like audio signal analysis and machine learning enable real-time identification of anomalies, allowing timely interventions [17]. The advantage of this approach is that it reduces maintenance costs, minimises downtime, and extends equipment lifespan [18].

Audio signal processing addresses some limitations of traditional diagnostic methods like vibration analysis [19] [20] or infrared thermography [21] [22] that require specialized sensors and direct access to machinery. Audio-based methods utilise non-intrusive microphones to capture sound emissions from equipment and are particularly useful in hazardous areas [23] [24]. Audio signals obtained from acoustic emission-based techniques have emerged as effective tools for diagnosing faults in power-generating systems [25] [26]. These sound signals originating from various mechanical activities, such as friction, impacts, and material deformation, which occur during the operation of power-generating sets, are used to identify and characterize mechanical faults like bearing wear, misalignments, cracks, and rotor imbalance [27]. Other common faults associated with generator sets are faults associated with the Carburetor [28] [29], valves [30], plugs, and exhaust systems.

Audio signal processing can be incorporated into machine learning (ML) for automating fault characterization by enabling the detection of patterns in complex datasets. ML algorithms (Fast Fourier Transform (FFT), Support Vector Machines (SVM) [31], Decision Trees [32] [33], K-Nearest Neighbors (KNN) [34] [35], [36], or Neural Networks [37], [38], [39] can process volumes of data, learn and distinguish between normal and faulty conditions [40] [41] This integration further strengthens the diagnostic process by leveraging advanced feature extraction techniques such as temporal and spectral feature extraction techniques, Mel-Frequency Cepstral Coefficients techniques, time-localized Fourier transforms (STFT), auditory-inspired cepstral descriptors (GFCCs), and wavelet transforms. The key features of audio signals that are relevant for fault detection include frequency, amplitude, and phase [42]. Each of these features provides insights into different aspects of the machinery's behaviour and can be crucial for identifying faults in their early stages.

A. Related Works

The robust capacity for feature extraction and classification of linear and non-linear relationships using machine learning (ML) algorithms has led to several proposals for the use of artificial intelligence (AI) methods in fault diagnosis. ML algorithms provide high flexibility and fault diagnosis performance [43]. ML algorithms such artificial neural networks (ANN) [44]; [45]; [46], decision tree (DT) [47], Bayes network [48], extreme learning machine (ELM) [49], K-nearest neighbors (KNN) [50] [51], linear discriminant analysis (LDA) [52], logistic regression (LR) [53], support vector machine (SVM) have been used for faults diagnosis and detection in transformers transformer [54].

Numerous machine learning application have been geared towards fault diagnosis in ship or aircraft and in diesel generators such as ship diesel generator diagnosis using fuzzy logic [55], diesel generator diagnosis and fault detection in wind turbines using deep learning [56] [57], and synchronous generator fault diagnosis using ANN [58] [59].

[60] carried out a comparative analysis of three (3) machine learning models (Simple, ensemble, and gradient boost) developed for diagnosing faults in power generators using a customized generator fault database (GFDB). The data was pre-processed and hyperparameters selected while the performance of the models was evaluated using key performance metrics including accuracy, precision, recall, and F1-Score.

Their findings revealed that the gradient boost demonstrated superior detection of the class 3 and class 4 faults. Although the GB model showed excellent overall performance, it particularly misclassified class 1 and class 2 faults. Comparing the confusion matrices for both GB and decision tree (DT) models showed that GB achieved high accuracy (≥80%) for most fault types. The major limitation of the study was associated with not identifying negative cases correctly (specificity) with each fault class. Also, the research categorized the faults in a general manner as catastrophic failures and specific fault types 0, 3, 4, and 5, creating a gap in understanding the root causes of the faults. Thus limiting effective maintenance and troubleshooting in power-generating sets. Also, the use of a curated dataset is another significant limitation of the study.

The authors [61] proposed a system for machinery health monitoring during operation and an alert system for potential failures. The system was developed using noise signals collected from the electrical system of rotating machinery, such as electric motors, turbine generators, and bearing fault motors with microphones. The study demonstrates that mechanical faults in rotating machinery can be effectively diagnosed by analyzing the noise signals emitted in association with mechanical vibrations. The noise signal analysis focuses on vibration-induced noise signatures. The automated noise analysis system showed high efficacy in detecting abnormal conditions in machinery and providing early fault alarms. Additionally, the system offers the advantage of practical implementation without significantly increasing the size or power requirements of the monitored motors. While the system is effective in detecting faults, the study does not address fault classification, leaving the specific categorization of detected faults unexplored.

A fault diagnosis system using Electrical Signature Analysis (ESA) for operational synchronous generators (SGs) dynamically integrated into the active power grid within bulk electric systems was explored [62]. This technique is employed for predictive maintenance to enhance SG protection and reliability. The electrical signals were processed and analyzed using the FFT algorithm to detect significant changes indicative of faults. The methodology was tailored for fault detection in wound-rotor synchronous generators (SGs), with an emphasis on current signature analysis (CSA) over voltage signatures. The study identified operational defects and anomalies, such as stator winding imbalances and rotor misalignment, through spectral signature analysis in the frequency domain. The results demonstrate ESA's effectiveness in condition monitoring and fault detection for SGs connected to power systems. The deployed prototype identified two faults: Interphase Short Circuit in the Stator Windings circuits detected through an imbalance in electrical patterns, and rotor misalignments identified through frequency patterns of the rotor. The findings validate ESA's potential for non-invasive predictive maintenance of SGs within interconnected power systems. However, the system was limited to fault diagnosis in SGs within bulk electric systems, suggesting the use of artificial intelligence techniques to enhance system automation and diagnostics.

The proposed system by [63] utilized signal processing and machine learning to identify faults in induction motors, thereby mitigating industrial downtime and plant disturbances. MATLAB Simulink was used to generate the dataset for faults induced at different load conditions and severity levels. The 150,000 data points comprised variables encompassing electrical parameters (e.g., stator and rotor currents), active power consumption, rotational dynamics (slip, rotor angular velocity), and operational efficiency metrics (e.g., energy conversion efficiency). The experimental setup incorporated four distinct failure modes: conductive path interruption (open circuit), aberrant current pathways (short circuit), sustained overcurrent conditions (overload), and structural degradation of rotor elements (broken rotor bars). A fast Fourier transform (FFT) was used for feature extraction, and four classification algorithms—Decision Trees, Naïve Bayes, K-Nearest Neighbors (KNN), and Support Vector Classifier (SVC) — were employed for fault diagnosis. The system was not deployed in a real-world environment but was simulated in a MATLAB environment. The models were evaluated using key performance metrics, including predictive accuracy, sensitivity (also known as recall), and the F1 score. The results demonstrate that the Decision Tree algorithm had improved performance compared to the other models, achieving an accuracy of 92.1%. Naïve Bayes, KNN, and SVC achieved lower accuracies of 61.3%, 52%, and 63%, respectively.

3. Methodology

This section outlines the materials used to implement this work and describes the method's structure. A combination of hardware and software resources was utilized to accomplish this task. The list of materials used is presented below.

1) A mobile phone of the following specification was used for audio data collection, capturing signals from 25 5kVA power-generating systems under various fault and normal conditions. Phone Performance Capabilities Brand: Infinix Smart 8; Operating System: Android 11(Go edition) with HIOS 7.6; Chipset: MediaTek 6762 Hello P22 (12nm); CPU: Octa-core 2.0GHz Cortex-A53; GPU: PowerVR GE8320.
2) Laptop Specifications: HP, Windows 10 Pro, 11th Generation Intel® Core™ i5 processor, 16 GB memory; 256 GB SSD storage, 14″ diagonal FHD display, Intel® Iris® X^e Graphics for data processing, model training, and testing.
3) Jupyter Notebook Python software with a suite of specialized libraries including Scikit-learn, Librosa, Scipy, Spafe, Noise Reduce, and Pywavelets were used for audio signal processing, data pre-processing tools including Pandas and NumPy, Visualization tools like Matplotlib and Seaborn, feature extraction, noise reduction, and system development (Google Colab streamline experimentation).
4) System deployment was done using a Raspberry Pi 3 microcontroller, microphone sensors, communication modules (Wi-Fi), and an LCD module to implement and test the fault diagnosis system in real-world settings.

A structured methodology was used to develop a fault diagnosis and characterization system for power generators, as shown in Fig. 1.

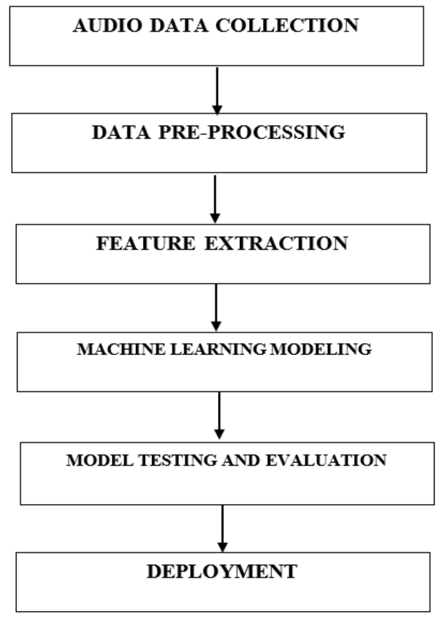

Figure 1. Block Diagram of System Methodology

A. Data Collection and Description

The audio data were collected from 25 running petrol-powered generators, using microphones and audio software on mobile phones. All the recordings were made in the city of Uyo, Nigeria, with an average duration of 1.5 minutes. The collected dataset recordings were categorised based on four common fault conditions: Exhaust, Plug, Carburettor, and Valve. Additionally, there is a category labeled as 'Normal', which indicates the normal operating condition of the generators with no faults. The recorded data is annotated with corresponding fault labels to facilitate supervised learning.

The faults identified for this work are defined as:

i. **Carburetor:** caused by dirt, fuel-related issues, air-fuel mixture problems, wear and tear, and improper maintenance.
ii. **Exhaust:** caused by blockages, leaks, corrosion, or damaged components like the muffler or exhaust pipe,

leading to poor performance, increased emissions, or excessive noise.

iii. **Valve:** Valve faults in a generator can result from improper timing, wear and tear, carbon buildup, or poor lubrication, leading to loss of compression, reduced power, and engine misfires.

iv. **Plug:** Plug faults in a generator, such as fouling, wear, or improper gap, can lead to weak or no spark, causing difficulty in starting misfires, or poor engine performance.

B. Signal Pre-Processing

The audio signals were cleaned, trimmed, and framed to remove noise, silent portions, and unwanted artifacts using the Audacity software. Exploratory data analysis (EDA) of the collected audio files was done using librosa, pydub, wave, os, and scipy.io.wavfile to reveal important information about the data collected before feature extraction.

A frame size of 100 milliseconds was used to segment the audio samples for this research with a 30% overlap between adjacent frames to prevent loss of vital information. This was done because signal discontinuities occur at the frame boundaries due to the windowing operation, which creates artificial frequencies.

C. Feature Extraction

In the feature extraction stage, both temporal and spectral were extracted from the time and frequency domains and used for training, model development, and testing. These features are presented below:

1) Root Mean Square (RMS) Energy: This feature serves as a statistical metric that provides the amplitude fluctuations of the audio time-varying signal. It assesses the energy content within acoustic waveforms. The equation is given in Equation 1

$$E_{RMS} = \frac{1}{N}\sum_{i=1}^{N} x_i^2 \quad (1)$$

Where x_i denotes the discrete temporal instances of the acoustic waveform, and N signifies the cardinality of the sampled dataset under analysis.

2) Zero Crossing Rate (ZCR): The Zero Crossing Rate (ZCR) is used to quantify the frequency of polarity transitions (positive to negative or vice versa) between consecutive waveform samples in an acoustic signal. A binary threshold function was used to output 1 (unity) when adjacent samples exhibit opposing polarities; otherwise, it outputs zero. These transitions provided insights into the noisiness and periodicity characteristics of the acoustic signals obtained. The Zero Crossing Rate (ZCR) was implemented using Equation 2.

$$ZCR(a) = \frac{1}{2}\sum_{i=2}^{n}|sign(a_i) - sign(a_{i-1})| \quad (2)$$

3) Continuous Wavelet Transform (CWT): Due to the non-stationary nature of acoustic signals, the CWT captures both transient (sudden bursts and clicks) and sustained features, which are necessary for analysis. The Continuous Wavelet Transform (CWT) extracted statistical features from the CWT coefficients, including the mean, variance, energy, entropy, skewness, and kurtosis, across the signal. These features provided the time-frequency representation (i.e., how the frequency content of an audio signal changes over time) of the signal using multi-resolution analysis (with resolutions at low frequencies and sharper detections at high frequencies) for input to the machine learning stage. Due to its localized nature, CWT is more effective at isolating features in noisy environments compared to other methods that employ global transformations, such as the FFT.

The continuous wavelet decomposition of the acoustic signal $x(t)$ is mathematically represented in Equation 3:

$$x_w(a,b) = \frac{1}{|a|^{\frac{1}{2}}}\int_{-\infty}^{\infty} x(t)\bar{\varphi}\left(\frac{t-b}{a}\right)dt \quad (3)$$

Where $\psi(t)$ represents the mother wavelet, a continuous, integrable function defined across both temporal and spectral domains, $\bar{\varphi}$ is the complex conjugate facilitating the generation of derived wavelet functions (daughter wavelets) through scaling ($a \in \mathbb{R}^+$) and translation ($b \in \mathbb{R}$) operations, and $x_w(a,b)$ is the resulting wavelet coefficient represented as a scalogram.

The scalogram output from Equation 3 is transformed using the Morlet wavelet as shown in Equation 4 into the time-frequency representation.

$$w(t) = \frac{1}{K\sigma}e^{-(\sigma t)^2}\cos(2\pi f_0 t) \quad (4)$$

where $w(t)$ is the Morlet wavelet function, f_0 is the centre frequency typically around 0.8125 in normalized units and bandwidth σ.

4) Mel-Frequency Cepstral Coefficients: the mel-frequency cepstral coefficients (MFCCs) features were obtained first by applying pre-emphasis to the audio signal to amplify the energy of higher frequencies by adjusting the tilt of the spectrum. This step gives added robustness to our model because the energy content of higher frequency components of the generator audio is increased. The pre-emphasis is implemented using the general equation expressed in Equation 5.

$$s(t) = x(t) - \alpha x(t-1) \quad (5)$$

where α is a dimensionless factor typically about 0.97 and x(t) the original signal.

The commonly used Hamming window function was applied to each framed signal to ensure smooth transitions to zero at the ends, thereby reducing artifacts in time-frequency representations, minimizing spectral leakage, improving frequency accuracy, and producing cleaner spectrograms. This is usually done before frequency analysis.

The Hamming window is expressed in Equation 6:

$$w(t) = 0.54 - 0.46\cos\left(\frac{2\pi t}{N-1}\right) \quad (6)$$

where t ranges from 0 to $N - 1$, and N is the length

The frequency spectrum of each windowed frame of the acoustic signal was obtained by applying the Fast Fourier Transform (FFT) to each windowed frame. The Fast Fourier Transform (FFT) is used to compute both the Discrete Fourier Transform (DFT) and its inverse. The DFT converts a time-domain signal into its frequency-domain representation by resolving it into sinusoidal components of varying frequencies. The FFT is implemented as shown in Equation 7.

$$X(k) = \sum_{n=0}^{N-1} x(n) \cdot e^{-i\frac{2\pi kn}{N}} \tag{7}$$

Where $X(k)$ represents the magnitude of the FFT.

After applying the FFT to each windowed frame, we obtained the complex-valued frequency components. The absolute value of the FFT for the windowed frame is obtained as shown in Equation 8:

$$|X(k)| = \sqrt{\mathcal{R}_e(X(k))^2 + \mathcal{I}_m(X(k))^2} \tag{8}$$

Where $X(k)$ is the FFT of the windowed frame, and $\mathcal{R}_e$(X(k)) and $\mathcal{I}_m$(X(k)) are the real and the imaginary components, respectively.

The power distribution of each frequency component within each windowed frame is computed using the power spectrum and is presented in Equation 9.

$$P(k) = \frac{1}{N}|X(k)|^2 \tag{9}$$

Where N denotes the total count of discrete data points within each temporal analysis window during signal processing. To obtain the MFCC of each signal, the Filter-Bank Operation was implemented. This step measured the energy across different frequency bands, spaced according to the Mel scale, which is a perceptual scale representing higher frequencies with lower resolution. This was achieved through the use of Mel filter banks consisting of overlapping bandpass filters with triangular magnitude responses strategically positioned across the signal's spectral energy distribution. These filters are spaced linearly across lower frequency ranges to approximate human auditory perception's non-linear frequency resolution, transitioning to logarithmic spacing in higher frequency regions to align with the Mel scale's psychoacoustic properties.

Equation 10 defines the Mel scale as:

$$m(f) = 2595.\log_{10}\left(1 + \frac{f}{700}\right) \tag{10}$$

Where f is the given frequency in Hz.

The logarithm energy is obtained by multiplying the power spectrum by each filter bank and summing the result to obtain the total energy in each Mel band given by Equation 11.

$$E_m = \sum_{k=f_i}^{f_{i+1}} P(k) \cdot H_m(k) \tag{11}$$

where E_m is the energy in the mth Mel filter, $\mathcal{P}(k)$ is the power spectrum at frequency k, and $H_m(k)$ is the Mel filter's magnitude response of the mth filter at frequency k.

The log-transformed power spectrum undergoes conversion into cepstral coefficients using the Discrete Cosine Transform (DCT), which serves as a type of inverse Fourier transform to convert the log-power spectrum from the spectral to the cepstral domain. This stage effectively decorrelates the features to enhance their suitability for pattern recognition and machine learning models. This process leverages the mathematical properties of the cepstral domain to isolate independent signal components, optimizing discriminative performance in audio analysis applications. The DCT compresses the signal information into the first few coefficients, making the features more compact and easier to model. This is shown in Equation 12.

$$C_n = \sum_{m=0}^{M-1} \log Energy_m \cdot \cos\left[\frac{\pi n}{M}\left(m + \frac{1}{2}\right)\right] \tag{12}$$

Where C_n denotes the n-th Mel-Frequency Cepstral Coefficient, capturing spectral characteristics in the cepstral domain, M represents the total number of triangular Mel-spaced filters applied to the power spectrum, and n defines the truncation limits for the cepstral coefficients, $\log Energy_m\ q$ uantifies the logarithmic energy output of the *m*-th Mel-frequency band, enhancing perceptual relevance.

D. *Machine Learning Algorithms (Model Training and Testing)*

The machine learning algorithms used in this work were the Support Vector Classifier (SVC), K-Nearest Neighbor (KNN), and Random Forest classifiers. The extracted features were split into a 70:30 ratio for training and testing the models, using a 10-fold cross-validation for model generalizability.

The Support Vector Machine (SVM) is a discriminative supervised learning model efficient in high-dimensional feature spaces. Its kernel-driven transformations enable robust classification of both linearly and non-linearly separable data distributions. It utilizes kernel tricks to solve non-linear problems by mapping the input features into a higher-dimensional space, where a linear separation can be achieved. Some kernels include linear, polynomial, radial basis function (RBF), and sigmoid.

$$min\left(\frac{1}{2}||\omega||^2 + C\sum_{i=1}^{n}\xi_i\right) \tag{13}$$

Subject to:

$$y_i(w.\phi(x_i) + b) \geq 1 - \xi_i,\ \xi_i \geq 0,$$

Where ϕ represents kernel-induced feature space transformation, ξ_i introduce flexibility by tolerating marginal classification errors, particularly for non-separable datasets, and C governs the trade-off between maximizing the classifier's margin and penalizing misclassified instances, ensuring robustness to overfitting. The hyper-parameter tuning of the SVC model was achieved using the parameters –

```
# Hyperparameter tuning
svc = SVC(probability=True)
param_grid={'C':[1,10,100,1000],'gamma':
[1,0.1,0.001,0.0001], 'kernel':['rbf']}
grid = GridSearchCV(svc, param_grid, refit=True,
verbose=3)
grid.fit(X_train, y_train)
print("Best Parameters:", grid.best_params_)
print("Best Estimator:", grid.best_estimator_)
```

The k-nearest neighbour's machine learning algorithm is a simple, effective, and instance-based non-parametric learning method used in this work for classification. This algorithm operates on the principle of similarity, leveraging the proximity of data points (measured by Euclidean distance) in a feature space to make predictions. The Euclidean distance metric used to quantify the similarity between instances is given in Equation 14.

$$(x, y) = \sqrt{\sum_{i=1}^{n}(x_i - y_i)^2} \tag{14}$$

The hyperparameter tuning phase of the KNN model was done using the parameters in the code –

```
# Hyperparameter tuning
k_range = list(range(1, 31))
param_grid = dict(n_neighbors=k_range)
grid_search_knn = GridSearchCV(knn, param_grid, cv=10, scoring='accuracy', return_train_score=False, verbose=3)
grid_search_knn.fit(X_train, y_train)
best_params = grid_search_knn.best_params_
print("Best Parameters:", best_params)
```

The ensemble-based Random Forest machine learning framework was used to synthesize predictions from multiple decision trees, thereby enhancing predictive accuracy and robustness. For classification, the prediction is given by Equation 15.

$$\bar{y} = argmax \sum_{b=1}^{B} I(h_b(x) = c) \tag{15}$$

where $h_b(x)$ is the prediction of the b-th tree.

The hyperparameter tuning phase of the random forest model was done using the parameters in the code –

```
#hyperparameter tuning
classifier = RandomForestClassifier()
param_grid = {
    'n_estimators': [100, 150],
    'max_depth': [10, 20],
    'min_samples_split': [5, 10],
    'min_samples_leaf': [2, 4]
}
```

E. Evaluation Metrics of Fault Diagnosis

The following are metrics used in evaluating the effectiveness of the fault diagnosis systems.

1) Accuracy (ACC)

This metric represents the ratio of correctly diagnosed faults to the total number of diagnosis attempts.

$$ACC = \frac{\text{Number of faults diagnosed}}{\text{Total Number of Diagnosis Attempts}}$$

2) Precision (Positive Predictive Value)

The precision metric measures the accuracy of positive diagnoses. It calculates the ratio of correctly diagnosed positive instances to the total number of instances diagnosed as positive. It protects the system from raising a false alarm.

$$\text{Precision} = \frac{\text{True Positives}}{\text{True Positives} + \text{False Positives}}$$

The precision metric says - out of the predicted fault cases, how many were actual faults?

3) Recall (Sensitivity)

Recall, which assesses the sensitivity of the system, was used to measure the proportion of actual positive instances that the system correctly diagnosed.

$$\text{Recall} = \frac{\text{True Positives}}{\text{True Positives} + \text{False Negatives}}$$

The recall metric says - out of all actual faults, how many did we correctly detect?

4) F1-Score

The F1-score metric is suitable for an audio-based fault diagnosis system because it balances the detection of actual faults and the avoidance of false alarms, especially under imbalanced and high-risk conditions. F1-score is the harmonic mean of precision and recall. It provides a balance between these two metrics.

$$\text{F1} - \text{Score} = \frac{\text{Precision} \times \text{Recall} \times 2}{\text{Precision} + \text{Recall}}$$

Since fault data is often unbalanced, the F1-score serves as a means to penalize models that ignore the minority class (faults) in favor of the majority class (normal conditions). It also provides a single, interpretable metric for comparing model performance under different training or feature extraction conditions. The F1 score ranges from 0 to 1, with a value of 1 indicating perfect precision and recall.

F. System Deployment

The deployment design for this research, which enables the real-time classification of faults in power-generating systems based on audio signals, is illustrated in the block diagram of Figure 2. The system operates through the input stage, utilizing sound recording, the intermediary stage with signal processing, and the output stage, which involves user visualization. The system design is structured in such a manner that once it is powered on, it initiates a sequence of operations that involves capturing audio signals by recording, processing them through the machine learning model (signal processing and classification), and displaying the fault diagnoses (user interpretation) for the power-generating sets.

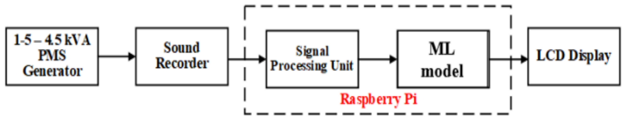

Figure 2. Block Diagram of System Prototype

4. Results and Discussion

In this section, the results of the experiments carried out are presented and discussed under each subsection.

A. Waveforms of Generator Audio Signals and Spectrograms.

Fig. 3 shows the waveform visualizations of the generator audio signals. They exhibit distinct temporal characteristics and variations in amplitude and frequency patterns associated with different fault conditions. These waveforms were pre-processed, and features were extracted for model development and used for diagnosing generator faults. The spectral signatures, which show the distinct temporal characteristics and variations in amplitude and frequency patterns of the audio signals, are presented in Fig. 4.

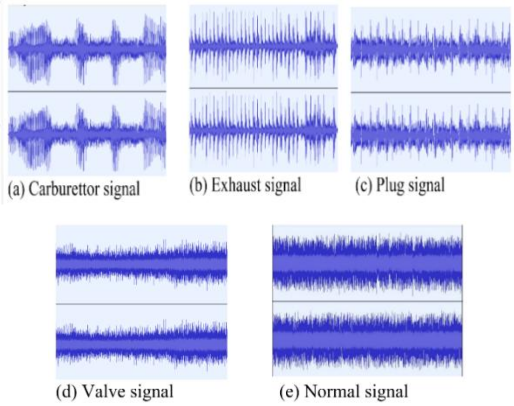

Figure 3. Waveforms of Recorded Generator Audio Fault Signals

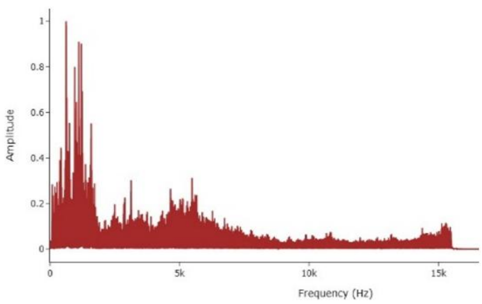

(a) Carburetor signal

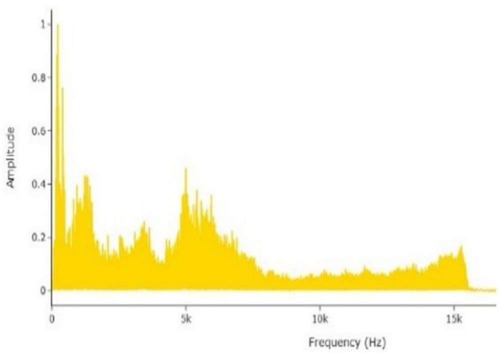

(b) Exhaust signal

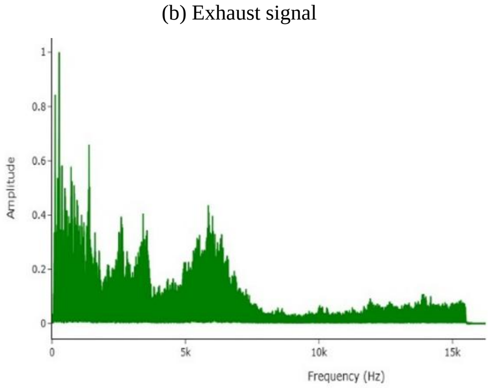

(c) Plug signal

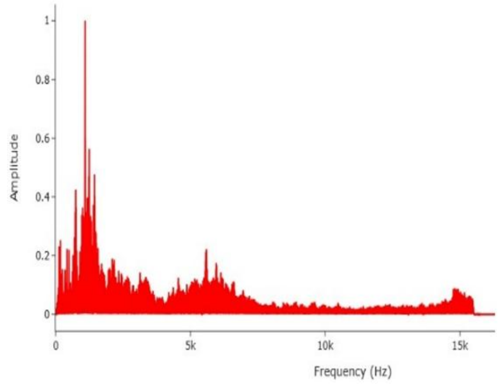

(d) Valve signal

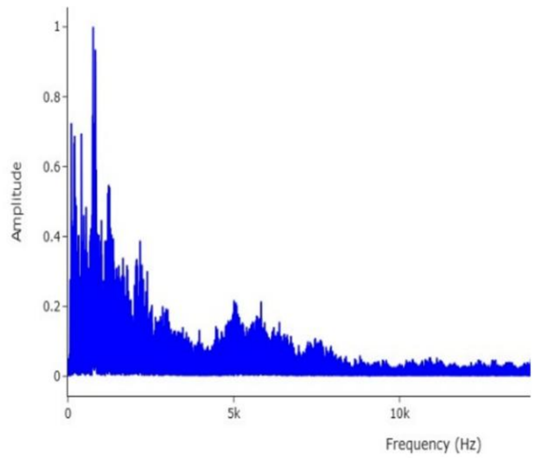

(e) Normal signal

Figure 4. Spectral Signatures of Recorded Generator Audio Fault Signals

B. Performance Evaluation of Machine Learning Models

The performance of the developed models was evaluated using the confusion matrix, accuracy, precision, recall, and F1-score metrics under two broad categories: without hyper-parameter tuning and with hyper-parameter tuning. The results obtained from the experiments are presented in the following sub-sections.

1) Performance Metrics without Hyperparameter Tuning.

Table 1 summarizes the overall performance metrics—accuracy, precision, recall, and F1-score—for three machine learning models: Random Forest, K-Nearest Neighbors (KNN), and Support Vector Classifier (SVC). These metrics provide an overview of model effectiveness in handling multi-class classification across five categories: Carburetor, Exhaust, Plug, Valve, and Normal. Figure 5 shows the confusion matrices for KNN, Random Forest, and SVC, respectively, which break down the correct and incorrect classifications for each fault category.

Table 1. Performance Metrics without Hyperparameter Tuning

Model	Accuracy	Precision	Recall	F1-Score
Random Forest	85%	85%	85%	85%
KNN	82%	82%	82%	82%
SVC	83%	83%	83%	83%

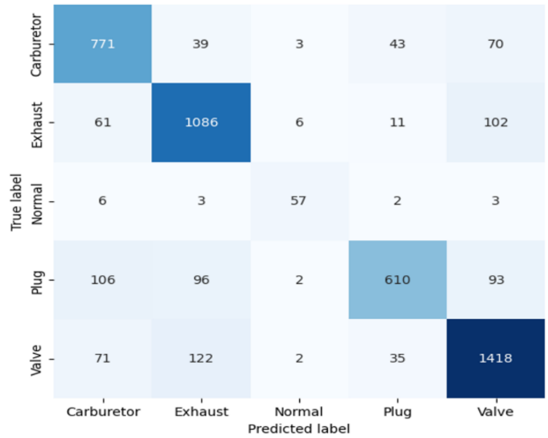

(a) KNN Model

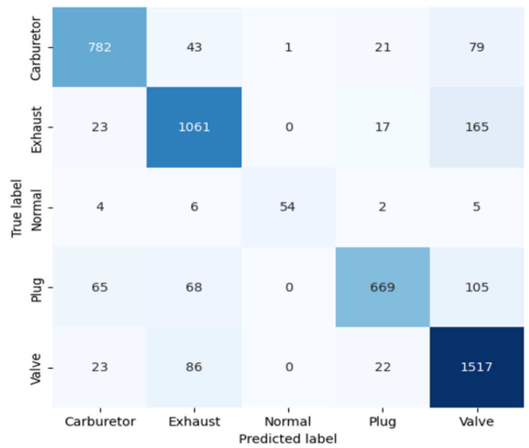

(b) Random Forest

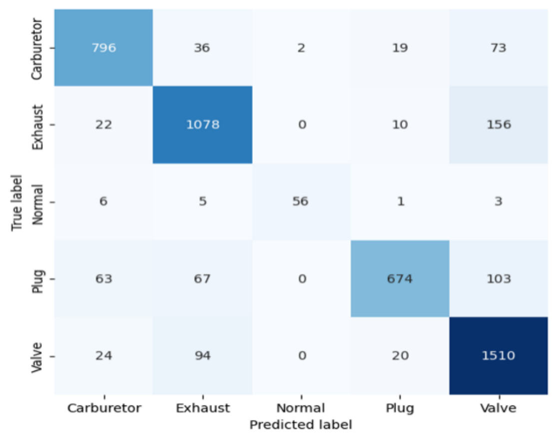

(c) SVC

Figure 5. Confusion Matrices for Machine Learning Models without Hyperparameter Tuning

Each row of the confusion matrices in Figure 5 represents the actual (true) class, each column represents the predicted class, and the diagonal values show correct predictions. The classes are the Carburetor, Exhaust, Normal, Plug, and Valve.

KNN Model

For the KNN model without hyper-parameter tuning in Figure 5(a), the following correct predictions - Carburetor: 771, Exhaust: 1,086, Normal: 57, Plug: 610 and Valve: 1,418.

The off-diagonal values are the model's miscalculations, and for the KNN model, the Carburetor was misclassified as Exhaust 39 times, Plug 43 times, and Valve 70 times; the Exhaust was misclassified as Carburetor 61 times and Valve 102; the Normal operating condition was misclassified as: Carburetor: 6 times and Exhaust: 3 times; the Plug fault was misclassified as: Carburetor: 106 times, Exhaust: 96 times and Valve: 93; and the Valve fault was misclassified as: Exhaust: 122 times and Carburetor: 71 times.

From the results of predictions made using the confusion matrix to evaluate True Positives, it was observed that -

i. **The Valve and Exhaust classes** had high true positive counts of 1,418 and 1,086, respectively, indicating the model performs well for these classes.
ii. **The Normal** class had the lowest true positive count of 57 and was often misclassified.
iii. **Plug** faults were frequently misclassified as Carburetor and Exhaust faults most especially.
iv. **The Carburetor class** had moderate performance with the KNN model and was misclassified most of the time as the Valve and Plug classes.

Random Forest Model

The Random Forest model accurately predicted the sample classes for the following numbers of instances: Carburetor (782), Exhaust (1,061), Normal (54), Plug (669), and Valve (1,517), as shown in Figure 5(b).

The miscalculations, as shown by the off-diagonal values, occurred as follows– the Carburetor was misclassified as Exhaust 43 times, Plug 21times, and Valve 79 times; the Exhaust was misclassified as Carburetor 23 times, Plug 17 times, and Valve 165 times; Normal was misclassified as: Carburetor: 4 times, Exhaust: 6 times, Plug: 2 times and Valve: 5 times; Plug fault was misclassified as: Carburetor: 65 times, Exhaust: 68 times and Valve: 105 times; Valve was misclassified as: Carburetor: 23 times, Exhaust: 86 times and Plug: 22 times.

The performance of the Random Forest model showed the following instances of high-accuracy classes –

i. **Valve**: 1,517 correct
ii. **Plug**: 669 correct
iii. **Exhaust**: 1,061 correct

SVC Model

From Figure 5(c), the SVC model showed the following correct predictions of fault cases - Carburetor: 796, Exhaust: 1,078, Normal: 56, Plug: 674, and Valve: 1,510.

The instances of misclassified faults by the SVC model include the following -

Carburetor faults were misclassified as Exhaust 36 times and misclassified as Valve 73 times; Exhaust faults were misclassified as Carburetor 22 times and misclassified as Valve 156 times;

Normal operating conditions were misclassified as Carburetor: 6 times, Exhaust: 5 times, Plug: 1 times and misclassified as Valve: 3 times;

The plug faults were misclassified as Carburetor faults 63 times, misclassified as Exhaust faults 67 times, and Valve faults 103 times, and

The valve faults was misclassified as Carburetor faults: 24 times, misclassified as Exhaust faults: 94 times, and misclassified as Plug faults: 20 times.

The SVC model showed performances with high True Positives across all classes, especially for Valve faults with 1,510 correct diagnoses, Exhaust with 1,078, and Plug with 674 correct diagnoses. The Normal class had 56 correct, which is significant considering that it was mostly underrepresented and harder to classify.

Table 2 shows a summarized comparison of the performance metrics, Precision, Recall, and F1-score, used to assess the performance of the three (3) models, KNN, Random Forest (RF), and SVC models for each fault class.

Table 2. Comparison of Precision, Recall and F1 across untuned KNN, Random Forest(RF) and SVC models for each fault class

CLASS	KNN Precision	KNN Recall	KNN F1	RF Precision	RF Recall	RF F1	SVC Precision	SVC Recall	SVC F1
Carburettor	0.760	0.833	0.794	0.872	0.844	0.858	0.874	0.860	0.867
Exhaust	0.807	0.858	0.832	0.839	0.838	0.839	0.842	0.852	0.847
Normal	0.814	0.803	0.809	0.982	0.761	0.857	0.966	0.789	0.868
Plug	0.870	0.673	0.759	0.915	0.738	0.817	0.931	0.743	0.826
Valve	0.841	0.860	0.851	0.811	0.921	0.862	0.818	0.916	0.865

From the performances presented in Table 2, SVC outperforms both KNN and RF in F1-score across most classes;

Random Forest had the highest recall for valves with very good precision for Normal.

KNN consistently underperformed compared to SVC and RF, especially in recall for Plug and precision for Carburetor.

The SVC model achieved the most balanced performance across all classes, making it suitable for real-world deployment in this fault diagnosis task.

2) Performance Metrics with Hyperparameter Tuning.

Hyperparameter tuning was introduced, and the models were tested for classifying Carburettor, Exhaust, Plug, and Valve faults, as well as Normal operation. The models' performances, evaluated across the evaluation metrics, and the overall percentage performances for each model are shown in Table 3. Fig. 6 shows their respective confusion matrices.

Table 3. Performance Metrics after Hyperparameter tuning

Model	Accuracy	Precision	Recall	F1-Score
Random Forest	85.4%	86%	85%	85%
KNN	82%	82%	82%	82%
SVC	87%	87%	87%	87%

The performances of the hyperparameter-tuned KNN, Random Forest, and SVC models from the confusion matrices in classifying audio signals obtained from the petrol-powered generator set into the five main categories of Carburetor, Exhaust, Normal, Plug, and Valve are summarized in Table 4(a), 4(b) and 4(c).

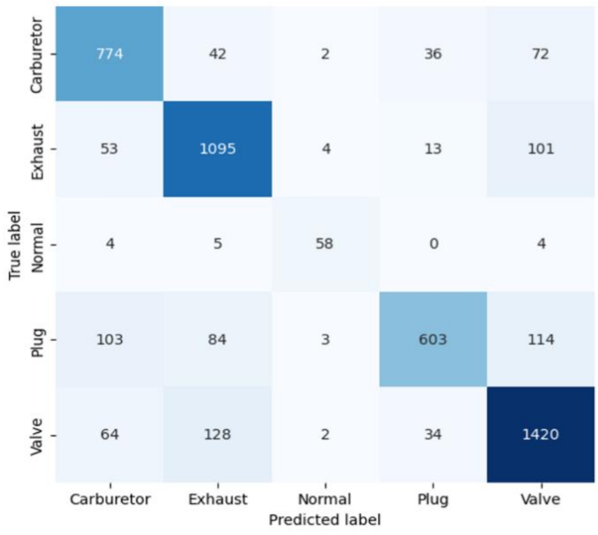

(a) KNN

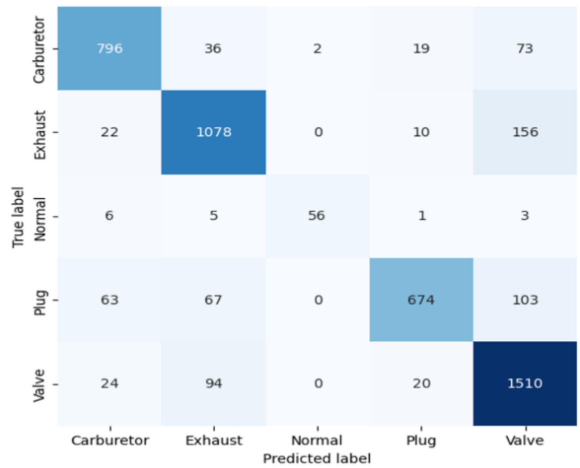

(b) Random Forest

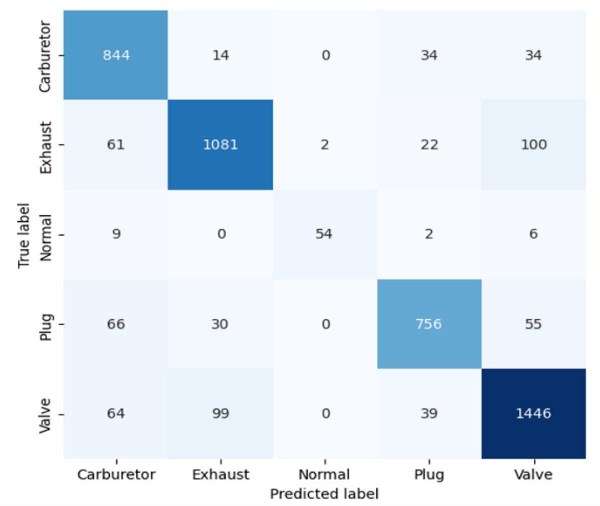

(c) SVC

Figure 6. Confusion Matrices for Machine Learning Models with Hyperparameter Tuning

Table 4(a). Overview of KNN Model performance from the confusion matrix

ACTUAL /PREDICTED	CARBURETOR	EXHAUST	NORMAL	PLUG	VALVE
CARBURETOR	774	42	2	36	72
EXHAUST	53	1095	4	13	101
NORMAL	4	5	58	0	4
PLUG	103	84	3	603	114
VALVE	64	128	2	34	1420

Table 4(b). Overview of Random Forest Model performance from the confusion matrix

ACTUAL /PREDICTED	CARBURETOR	EXHAUST	NORMAL	PLUG	VALVE
CARBURETOR	796	36	2	19	73
EXHAUST	22	1078	0	10	156
NORMAL	6	5	56	1	3
PLUG	63	67	0	674	103
VALVE	24	94	0	20	1510

Table 4(c). Overview of SVC Model performance from the confusion matrix

ACTUAL/PREDICTED	CARBURETOR	EXHAUST	NORMAL	PLUG	VALVE
CARBURETOR	844	14	0	34	34
EXHAUST	61	1081	2	22	100
NORMAL	9	0	54	2	6
PLUG	66	30	0	756	55
VALVE	64	99	0	39	1446

The Valve fault was correctly classified 1420 times with very high precision/recall, the Exhaust fault was correctly classified 1095 correctly classified with low misclassification, and the model had 58 correct classifications for Normal 58 correctly classified, though the total count seems lower (small class).

For the misclassified classes, Plug → Valve: 114 instances, Plug → Carburetor: 103 instances, Plug → Exhaust: 84 instances, and Valve → Exhaust: 128 misclassified.

The instances of correct classifications made for the five (5) classes were

i. **Valve**: 1510 (very strong performance)
ii. **Exhaust**: 1078 (minimal misclassification)
iii. **Normal**: 56 (very accurate for this small class)
iv. **Plug**: 674
v. **Carburetor**: 796

The instances of incorrect classifications made for the five (5) classes are

i. **Exhaust → Valve**: 156 misclassified
ii. **Plug → Carburetor/Exhaust**: 63 and 67 misclassified, respectively
iii. **Carburetor → Valve**: 73 misclassified

The instances of correct classifications by the SCV model are

i. Valve: 1446 correctly classified
ii. Exhaust: 1081 correctly classified
iii. Plug: 756 correctly classified – better than KNN, slightly lower than Random Forest.
iv. Normal: 54 correctly classified
v. Carburetor: 844 correctly classified

The instances of misclassifications are listed below

i. Valve → Exhaust: 99 misclassified
ii. Exhaust → Valve: 100 misclassified
iii. Plug → Carburetor: 66 misclassified
iv. Carburetor → Valve/Plug: 34 each

Table 5. Comparison of Precision, Recall, and F1 across Hyper-parameter tuned KNN, Random Forest(RF), and SVC models for each fault class

CLASS	KNN Precision	KNN Recall	KNN F1	RF Precision	RF Recall	RF F1	SVC Precision	SVC Recall	SVC F1
Carburettor	0.77	0.79	0.78	0.82	0.82	0.82	0.85	0.84	0.84
Exhaust	0.82	0.9	0.86	0.84	0.89	0.86	0.87	0.89	0.88
Normal	0.87	0.45	0.59	0.87	0.45	0.59	0.84	0.52	0.64
Plug	0.73	0.74	0.73	0.79	0.8	0.8	0.8	0.88	0.87
Valve	0.82	0.89	0.85	0.85	0.89	0.87	0.85	0.89	0.87

The results from Table 5 provide the following insights –

The SVC model exhibits an overall balanced performance, particularly in classifying Plug and carburetor faults, as well as normal operation.

The Random Forest model had the highest F1 score (0.87) for classifying the Valve fault.

KNN was the worst-performing model, with multiple misclassifications of the Normal condition and the Plug faults.

All the models had a low recall score for the Normal, indicating challenges in its classification.

True Positives (TP) represent the instances where the model accurately predicts the presence of a specific generator fault. TP directly impacts the Precision, Recall, and F1-score metrics, reflecting how well the models can diagnose faults from generator audio analysis. Table 6 shows the TP for each model and each class.

Table 6. Overall True Positives (TP) for KNN, Random Forest, and SVC models

Metric / Class	KNN	Random Forest	SVC
Valve TP	1420	1510	1446
Plug TP	603	674	756
Exhaust TP	1095	1078	1081
Normal TP	58	56	54
Carburetor TP	774	796	844
Overall Confusion	Highest (esp. Plug)	Moderate	Lowest among three

A high true positive (TP) rate means the system reliably identifies real faults, while a low true positive rate implies that the model misses actual faults, risking generator damage.

C. Machine Learning Models Comparative Analysis

The comparative performances of the Random Forest, K-Nearest Neighbors (KNN), and Support Vector Classifier (SVC) machine learning models, with and without hyperparameter tuning, along with their respective percentage improvements, are presented in Table 7.

Table 7. Comparative Accuracy Performance of Machine Learning Models

Model	Before Hyperparameter Tuning	After Hyperparameter Tuning	Improvement
Random Forest	85%	85.4%	0.47%
KNN	82%	82%	0%
SVC	83%	87%	4.8%

From the results of hyperparameter tuning, SVC exhibited the most notable improvement, with accuracy rising to 87% (a 4.8% increase) compared to Random Forest and K-Nearest Neighbors (KNN).

The best overall performance of the machine learning models presented in Table 7, used in this work, is compared with the work of other authors in Table 8.

Table 8. Comparative Analysis of the Developed Models and Related Works

Model	Accuracy	Source
Random Forest	85.4%	Current work
Random Forest	85%	Amaya-Sanchez et al. (2024)
KNN	82%	Current work
KNN	52%	Samiullah et al. (2024)
KNN	66%	Amaya-Sanchez et al. (2024)
SVC	87%	Current work
SVC	63%	Samiullah et al. (2024)
SVC	62%	Amaya-Sanchez et al. (2024)

Compared to related works, the developed SVC model achieved significantly higher accuracy than those reported by Samiullah et al. (2024) and Amaya-Sanchez et al. (2024), which recorded accuracies of 63% and 62%, respectively. Likewise, the developed KNN model, with an accuracy of 82%, outperformed the models in the same studies, which achieved accuracies of 52% and 66%. This improvement is likely due to the quality of data collected and the signal processing approach used.

D. Results for Real-Time Deployment and Testing

Figure 7. Accuracy Results of Different Faults Diagnoses for 2 Power Generators

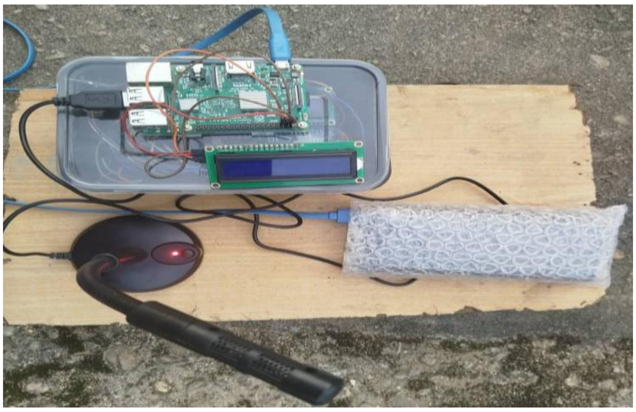

Figure 8. Picture of System Prototype

The real-time performance evaluation of the developed machine learning-based generator fault diagnosis and characterization system was conducted using two different generators for each fault condition. The results of the diagnosed faults and the corresponding percentage accuracy were displayed on the LCD screen, as illustrated in Fig. 7. Fig. 8 is the pictorial view of the system prototype.

E. Summary

The experimental analysis presented in this study focused on developing a machine learning-based fault diagnosis and characterization system for power-generating sets. The proposed approach utilized features extracted from a customized audio signal dataset collected from 25 5kVA petrol-powered generator sets to train and test the K-Nearest Neighbors (KNN), Random Forest (RF), and Support Vector Classifier (SVC) machine learning algorithms. The performance of the models was evaluated using key performance metrics—accuracy, precision, recall, and F1-score—with k-fold cross-validation (k=10) to ensure generalizability and a confusion matrix was used to derive performance measures for each condition. Five (5) fault conditions were studied and diagnosed -: Carburettor, Exhaust, Plug, Valve, and Normal operations. The results obtained were presented and discussed under three main areas: signal visualization and feature analysis, performance evaluation with and without hyperparameter tuning, and comparative analysis with existing studies. The waveform and spectral signature analyses of generator audio signals revealed temporal and frequency domain patterns unique to each fault category: Carburettor, Exhaust, Plug, Valve, and Normal operations. The performance Evaluation of Models showed that without hyperparameter Tuning, Accuracy: RF (85%) > SVC (83%) > KNN (82%); with hyperparameter Tuning, Accuracy Improvement: SVC had the highest improvement (+4.8%), reaching 87%, Model Accuracy: SVC (87%) > RF (85.4%) > KNN (82%). For the comparative analysis, the effect of hyperparameter tuning showed the most substantial improvement in SVC accuracy, validating the importance of model optimization. In the external benchmarking, the SVC model in this research (87%) exceeded the SVC models from Samiullah (63%) and Amaya-Sanchez (62%). Similar improvements were observed for RF and KNN models.

5. Conclusions and Recommendations

In this work, experiments were carried out to develop and test three machine learning (3) models for the diagnosis and characterization of three (3) mechanical faults, one (1) electrical fault, and Normal operation for power-generating sets. The fault features were extracted from the audio signals of the customized dataset, which was collected from 25 5kVA petrol-powered generator sets. The results obtained from testing the models showed that the models performed better with hyper-parameter tuning, especially the SVC. The SVC model consistently performed better than the other two (2) models across most categories, as well as the external benchmarks used. This outstanding performance is made possible because SVC can handle high-dimensional audio signals by separating the classes using an optimal hyperplane. It also uses the appropriate kernel and bias versus variance balance parameters. It is less affected by noise and can model complex non-linear boundaries, unlike basic Random Forests.

Suggestions for further work

To enhance the robustness of the fault detection system, future work could expand the dataset to include a broader range of fault conditions and generator types.

A multi-modal fault diagnosis system can be created by combining acoustic signal processing with other sensor data, such as vibration and/or temperature data. This will provide more comprehensive information about generator behaviour under fault conditions.

All the models performed better with hyper-parameter tuning which suggests that there is room for further optimization. In addition, more advanced models can be explored.

In this work, the study was limited to twenty-five 5kVA generator set. For better generalizability, studies can be expanded to accommodate more generator types and brands.

Our ML system was working well in controlled tests, however, more work investigating real-time deployment frameworks and edge-based solutions to assess feasibility and responsiveness in practical settings with respect to latency, actual hardware deployement and performance reliability under noisy real-world conditions.

The scope of this work is in traditional machine learning models. Additional deep learning models (e.g., ANNs, CNNs or LSTMs) to compare performance against these and other classical ML algorithms can be explored especially for temporal and spectral audio features.

REFERENCES

[1] K. Benyounes, M. Benbouzid and D. Diallo, "Advanced fault detection and diagnosis for gas turbine engines.," *IEEE Transactions on Industry Applications,*, vol. 49, no. 1, pp. 407-417, 2013.

[2] W. Yang, P. J. Tavner, C. J. Crabtree, Y. Feng and Y. Qiu, "Wind turbine condition monitoring: technical and commercial challenges," *Renewable Energy,* vol. 62, pp. 233-242, 2018.

[3] P. Henriquez, J. B. Alonso, M. A. Ferrer and C. M. Travieso, "Review of automatic fault diagnosis systems using audio and vibration signals.," *IEEE Transactions on systems, man, and cybernetics: Systems,* vol. 44, no. 5, pp. 642-652, 2013.

[4] Z. Li, Y. Zhang and J. Wang, "An overview of power generating set reliability," *Energy Reports,,* vol. 1, pp. 110-115, 2015.

[5] E. Elbouchikhi, H. Ziar, V. Choqueuse and M. Benbouzid, "A robust fault detection approach for gas turbine engines using wavelet transform and support vector machines," *Energy,* vol. 190, p. 116308., 2020.

[6] L. Tang, H. Tian, H. Huang, S. Shi and Q. Ji, "A survey of mechanical fault diagnosis based on audio signal analysis," *Measurement,* vol. 220, p. 113294, 2023.

[7] R. Kothamasu, S. H. Huang and W. H. VerDuin, "System health monitoring and prognostics—a review of current paradigms and practices," *International Journal of Advanced Manufacturing Technology,* vol. 28, no. (9-10), pp. 1012-1024., 2006.

[8] A. K. S. Jardine, D. Lin and D. Banjevic, "A review on machinery diagnostics and prognostics implementing condition-based maintenance.," *Mechanical Systems and Signal Processing,* vol. 20, no. 7, pp. 1483-1510., 2003.

[9] A. Senanayaka, P. Lee, N. Lee, C. Dickerson, A. Netchaev and S. Mun, "Enhancing the accuracy of machinery fault diagnosis through fault source isolation of complex mixture of industrial sound signals," *The International Journal of Advanced Manufacturing Technology,* vol. 133, no. 11, pp. 5627-5642, 2024.

[10] S. Delvecchio, P. Bonfiglio and F. Pompoli, "Vibro-acoustic condition monitoring of Internal Combustion Engines: A critical review of existing techniques.," *Mechanical Systems and Signal Processing,* vol. 99, pp. 661-683, 2018.

[11] Z. Qiao, Y. Lei and N. Li, "Applications of stochastic resonance to machinery fault detection: A review and tutorial.," *Mechanical Systems and Signal Processing,* vol. 122, pp. 502-536, 2019.

[12] Y. Li, J. Zhang and J. Lee, "A data-driven approach for multi-sensor health management in the presence of sensor failures.," *Journal of Manufacturing Science and Engineering,* vol. 136, no. 2, p. 021014, 2014.

[13] H. Zhou, C. Sun and S. Yang, "Fault diagnosis of power generation equipment: A comprehensive survey.," *IEEE Transactions on Industrial Electronics,,* vol. 63, no. 6, pp. 3454-3466., 2016.

[14] M. M. Zaben, M. Y. Worku, M. A. Hassan and M. A. Abido, "Machine learning methods for fault diagnosis in ac microgrids: A systematic review," *IEEE access,* vol. 12, pp. 20260-20298, 2024.

[15] J. Hare, X. Shi, S. Gupta and A. Bazzi, "Fault diagnostics in smart micro-grids: A survey. Renewable and Sustainable Energy," *Reviews,* vol. 60, pp. 1114-1124, 2016.

[16] H. Habibi, I. Howard and S. Simani, "Reliability improvement of wind turbine power generation using model-based fault detection and fault tolerant control: A review.," *Renewable energy,* vol. 135, pp. 877-896, 2019.

[17] O. AlShorman, M. Irfan, M. Masadeh, A. Alshorman, M. A. Sheikh, N. Saad and S. Rahman, "Advancements in condition monitoring and fault diagnosis of rotating machinery: A comprehensive review of image-based intelligent techniques for induction motors.," *Engineering Applications of Artificial Intelligence,* vol. 130, p. 107724, 2024.

[18] C. L. Melchor-Hernández, F. Rivas-Dávalos, S. Maximov, V. H. Coria and J. L. Guardado, "A model for optimizing maintenance policy for power equipment," *International Journal of Electrical Power and Energy Systems,* vol. 68, pp. 304-312, 2015.

[19] J. Feldman, B. M. Hanrahan, S. Misra, X. Z. Fan, C. M. Waits, P. D. Mitcheson and R. Ghodssi, "Vibration-based diagnostics for rotary MEMS," *Journal of Microelectromechanical Systems,* vol. 24, no. 2, pp. 289-299, 2015.

[20] T. O. Ajewole, B. M. Ojuola, A. A. Olawuyi, O. D. Momoh and O. Olukayode, "Application of machine learning to prediction of turbine rotor vibration in steam power plant.," *Journal of Energy and Safety Technology (JEST),* pp. 1-9, 2023.

[21] S. Bagavathiappan, B. B. Lahiri, T. Saravanan, J. Philip and T. Jayakumar, "Infrared thermography for condition monitoring –A review.," *Infrared Physics and Technology,* vol. 60, pp. 35-55, 2013.

[22] G. K. Balakrishnan, C. T. Yaw, S. P. Koh, T. Abedin, A. A. Raj, S. K. Tiong and C. P. Chen, "A review of infrared thermography for condition-based monitoring in electrical energy:Applications and recommendations," *Energies,* vol. 15, no. 16, p. 6000, 2022.

[23] Z. Hameed, Y. S. Hong, Y. M. Cho, S. H. Ahn and C. K. Song, "Condition monitoring and fault detection of wind turbines and related algorithms: A review.," *Renewable and Sustainable energy reviews,* vol. 13, no. 1, pp. 1-39, 2009.

[24] M. Tang, Q. Zhao, H. Wu, Z. Wang, C. Meng and Y. Wang, "Review and perspectives of machine learning methods for wind turbine fault diagnosis.," *Frontiers in Energy Research,* vol. 9, p. 751066, 2021.

[25] Y. Merizalde, L. Hernández-Callejo, O. Duque-Perez and R. A. López-Meraz, "Fault Detection of Wind Turbine Induction Generators through Current Signals and Various Signal Processing Techniques," *Applied Sciences,* vol. 10, no. 21, p. 7389, 2020.

[26] M. S. Nashed, J. Renno and M. S. Mohamed, "Fault classification using convolutional neural networks and color channels for time-frequency analysis of acoustic emissions.," *Journal of Vibration and Control,* vol. 30, no. 9-10, pp. 2283-2300, 2024.

[27] P. Gangsar and R. Tiwari, "Signal-based condition monitoring techniques for fault detection and diagnosis of induction motors: A state-of-the-art review.," *Mechanical systems and signal processing,* vol. 144, p. 106908, 2020.

[28] F. Akbalık, A. Yıldız, Ö. F. Ertuğrul and H. Zan, "Engine Fault Detection by Sound Analysis and Machine Learning.," *Applied Sciences,* vol. 14, no. 15, p. 6532, 2024.

[29] S. N. Dandare and S. V. Dudul, "Support vector machine based multiple fault detection in an automobile engine using sound signal," *Journal of Electronic and Electrical Engineering,* pp. ISSN, 0976-8106, 2012.

[30] X. Bi, S. Cao and D. Zhang, "Diesel engine valve clearance fault diagnosis based on improved variational mode decomposition and bispectrum," *Energies,* vol. 12, no. 4, p. 661, 2019.

[31] T. Jiang, J. L. Gradus and A. J. Rosellini, "Supervised machine learning: a brief primer.," *Behavior therapy,* vol. 51, no. 5, pp. 675-687, 2020.

[32] Z. Khan, A. Gul, A. Perperoglou, M. Miftahuddin, O. Mahmoud, W. Adler and B. Lausen, "Ensemble of optimal trees, random forest and random projection ensemble classification," *Advances in Data Analysis and Classification,* vol. 14, pp. 97-116, 2020.

[33] S. González, S. García, J. Del Ser, L. Rokach and F. Herrera, "A practical tutorial on bagging and boosting based ensembles for machine learning: Algorithms, software tools, performance study, practical perspectives and opportunities," *Information Fusion,* vol. 64, pp. 205-237, 2020.

[34] V. S. A. H. A. A. Prasatha, A. B. Hassanate, O. Lasassmehe, A. S. Tarawnehf, M. B. Alhasanatg and H. S. E. Salmane, "Effects of distance measure choice on knn classifier performance-a review.," *arXiv preprint arXiv:1708.04321,* p. 56, 2017.

[35] N. Ukey, Z. Yang, B. Li, G. Zhang, Y. Hu and W. Zhang, "Survey on exact knn queries over high-dimensional data space.," *Sensors,* vol. 23, no. 2, p. 629, 2023.

[36] R. K. Halder, M. N. Uddin, M. A. Uddin, S. Aryal and A. Khraisat, "Enhancing K-nearest neighbor algorithm: a comprehensive review and performance analysis of modifications.," *Journal of Big Data,,* vol. 11, no. 1, p. 113, 2024.

[37] S. T. Bhairnallykar and V. Narawade, "A Comprehensive Exploration of Convolutional Neural Network Architectures in Deep Learning.," in *In the International Conference on Recent Innovations in Computing,* Singapore, 2023.

[38] B. B. Traore, B. Kamsu-Foguem and F. Tangara, "Deep convolution neural network for image recognition.," *Ecological informatics,* vol. 48, pp. 257-268, 2018.

[39] I. R. I. Haque and J. Neubert, "Deep learning approaches to biomedical image segmentation," *Informatics in Medicine Unlocked,* vol. 18, p. 100297, 2020.

[40] Y. Lei, B. Yang, X. Jiang, F. Jia, N. Li and A. K. Nandi, "Applications of machine learning to machine fault diagnosis: A review and roadmap," *Mechanical systems and signal processing,* vol. 138, p. 106587, 2020.

[41] F. Calabrese, A. Regattieri, M. Bortolini and F. G. Galizia, "Data-Driven Fault Detection and Diagnosis: Challenges and Opportunities in Real-World Scenarios," *Applied Sciences,* vol. 12 , no. 18, p. 9212., 2022.

[42] G. Sharma, K. Umapathy and S. Krishnan, "Trends in audio signal feature extraction methods," *Applied Acoustics,* vol. 158, p. 107020, 2020.

[43] R. Arias and J. Mejia, "Health index for transformer condition assessment.," *IEEE Lat. Am. Trans.,* vol. 16, p. 2843–2849, 2018.

[44] T. Nagpal and Y. Brar, "Artificial neural network approaches for fault classification: Comparison and performance," *Neural Comput. Appl.,* vol. 25, p. 1863–1870, 2014.

[45] I. Taha, S. Dessouky and S. Ghoneim, "Transformer fault types and severity class prediction based on neural pattern-recognition techniques.," *Electr. Power Syst. Res.,* vol. 191, p. 106899, 2020.

[46] M. Mortada, S. Yacout and A. Lakis, "Power Transformer Fault Diagnosis Using Neural Network Optimization Techniques.," *Mathematics,* vol. 11, p. 4693, 2023.

[47] A. Menezes, M. Araujo, O. Almeida, F. Barbosa and A. Braga, "Induction of Decision Trees to Diagnose Incipient Faults in Power Transformers.," *IEEE Trans. Dielectr. Electr. Insul. ,* vol. 29, p. 279–286, 2022.

[48] A. Carita, L. Leite, A. Medeiros, R. Barros and L. Sauer, "Bayesian Networks applied to Failure Diagnosis in Power Transformer.," *IEEE Lat. Am. Trans. ,* vol. 11, p. 1075–1082, 2013.

[49] Q. Wu and H. Zhang, "A novel expertise-guided machine learning model for internal fault state diagnosis of power transformers.," *Sustainability,* vol. 11, p. 1562, 2019.

[50] A. Kumar and H. Vidya, "Application of k-Nearest Neighbor (kNN) Machine Algorithm for Transformer Fault Classification.," *Int. J. Adv. Sci. Technol.,* vol. 29, p. 8441–8448, 2020.

[51] P. Sekatane and P. Bokoro, "Partial Discharge Localization through k-NN and SVM.," *Energies ,* vol. 16, p. 7430, 2023.

[52] M. Mortada, S. Yacout and A. Lakis, "Fault diagnosis in power transformers using multi-class logical analysis of data.," *J. Intell. Manuf.,* vol. 25, p. 1429–1439, 2014.

[53] P. Mirowski and Y. Lecun, "Statistical machine learning and dissolved gas analysis: A review.," *IEEE Trans. Power Deliv.,* vol. 27, p. 1791–1799, 2012.

[54] G. Santamaria-Bonfil, G. Arroyo-Figueroa, M. Zuniga-Garcia, C. Azcarraga Ramos and A. Bassam, "Power Transformer Fault Detection: A Comparison of Standard Machine Learning and autoML Approaches.," *Energies ,* vol. 17, p. 77, 2024.

[55] M. Yucesan, V. Bashan, H. Demirel and M. Gul, "An interval type-2 fuzzy enhanced best–worst method for the evaluation of ship diesel generator failures.," *Eng. Fail. Anal.,* vol. 138, p. 106428, 2022 .

[56] H.-K. Jo, S.-H. Kim and C.-L. Kim, "Proposal of a new method for learning of diesel generator sounds and detecting abnormal sounds using an unsupervised deep learning algorithm," *Nucl. Eng. Technol,* vol. 55, p. 506–515, 2023.

[57] G. Helbing and M. Ritter, "Deep Learning for fault detection in wind turbines.," *Renew. Sustain. Energy Rev.,* vol. 98, p. 189–198, 2018.

[58] A. Nashee and A. Herez, "Neural Networks for Synchronous Generator Fault Diagnosis.," *IOP Conf. Ser. Mater. Sci. Eng.,* vol. 518, no. 39, p. 042015, 2019.

[59] O. Elfaki, W. Zhong and L. Hui, "Condition Monitoring and Faults Diagnosis for Synchronous Generator Using Neural Networks. Telkomnika Indones.," *J. Electr. Eng.,* vol. 12, p. 1196–1204, 2014, .

[60] Q. A. M. J. d. M. A.-L. A. A. R. M. O. A. a. A.-F. G. Amaya-Sanchez, "Fault Diagnosis in Power Generators: A Comparative Analysis of Machine Learning Models.," *Big Data and Cognitive Computing,,* vol. 8, no. 11, p. 145., 2024.

[61] Y. Altankhuyag and W. Hardt, "Automated noise analysis for fault detection.," *In IBS Scientific Workshop Proceedings,* vol. 4, pp. 19-24, 2017.

[62] C. P. Salomon, C. Ferreira, W. C. Sant'Ana, G. Lambert-Torres, L. E. Borges da Silva, E. L. Bonaldi and B. S. Torres, "A study of fault diagnosis based on electrical signature analysis for synchronous generators predictive maintenance in bulk electric systems," *Energies*, vol. 12, no. 8, p. 1506, 2019.

[63] M. A. H. Z. S. &. A. A. Samiullah, "Fault diagnosis on induction motor using machine learning and signal processing.," *arXiv preprint arXiv:2401.15417*, 2024.

Copyright © 2025 The Author(s). Published by Scientific & Academic Publishing
This work is licensed under the Creative Commons Attribution International License (CC BY). http://creativecommons.org/licenses/by/4.0/